JOURNAL OF MORPHOLOGY 277:196–203 (2016)

Pigment Cell Mechanism of Postembryonic Stripe Pattern Formation in the Japanese Four-Lined Snake

Arata Murakami,[1,2] Masami Hasegawa,[2] and Takeo Kuriyama[3]*

[1]*Kisarazu Sogo Senior High School, Ohta 3-4-1, Kisarazu, Chiba 292-0043, Japan*
[2]*Department of Biology, Faculty of Science, Toho University, Miyama 2-2-1, Funabashi, Chiba 274-8510, Japan*
[3]*Department of Environmental Science, Faculty of Science, Toho University, Miyama 2-2-1, Funabashi, Chiba 274-8510, Japan*

ABSTRACT Postembryonic changes in the dermal and epidermal pigment cell architecture of the striped and nonstriped morph of the Japanese four-lined snake *Elaphe quadrivirgata* were examined to reveal stripe pattern formation after hatching. The striped and nonstriped morphs were distinguishable at the hatching, suggesting that the basis of stripe pattern was formed during embryonic development. In the striped morph, the color of stripes changed from red-brown in juveniles to vivid dark-brown in adults, and density of dermal melanophore increased much more in the stripe than background dorsal scales with growth. This increase in density of dermal melanophore was accompanied not only by the increased epidermal melanophore density but also by the change in vertical structures of dermal melanophore. By contrast, the density of epidermal and dermal melanophore evenly increased over the dorsal scales in the nonstriped morph. Thus, the increased vividness of the stripe pattern after hatching is achieved through localized increase of melanophore density particularly in the stripe region but not over the whole dorsal scales. J. Morphol. 277:196–203, 2016.

KEY WORDS: ontogenetic color change; pigment cell; melanophores; xanthophores; iridophores

INTRODUCTION

A mechanistic approach is fundamental to understanding embryonic and postembryonic color pattern formation. Specifically, it is necessary to examine changes in pigment cell composition and the architectural arrangement of pigment cells during development (Kuriyama et al., 2006, 2013). An understanding of the pigment cell architectures of color polymorphisms may facilitate the identification of the genetic mechanisms that underlie color pattern formation (Olsson et al., 2013).

Reptilian sauropsids exhibit a wide variety of color patterns (Cooper and Greenberg, 1992; Allen et al., 2013; Olsson et al., 2013), and histological descriptions of the skin pigment cells of lizards, snakes, crocodiles, and tuataras (e.g., Morrison, 1995; Alibardi, 2011, 2012) have demonstrated that these color patterns are produced by the vertical architectures of pigment cells (chromatophores), including black melanophores, yellow xanthophores, and iridescent iridophores (Kuriyama et al., 2006; Saenko et al., 2013). The spatial arrangement of these chromatophores produces a variety of color patterns, from simple uniform brown or green to complex patterns, such as ringed, banded, striped, speckled, blotched, chevron, diamond, and zigzag arrangements (e.g., Bechtel, 1978; Wolf and Werner, 1994). Despite the rich diversity of color patterns in reptilian sauropsids (Wilson et al., 2007), surprisingly few studies have examined the pigmentation mechanisms underlying ontogenetic changes in color pattern (Chang et al., 2009; Kronforst et al., 2012).

The pigmentation mechanisms that determine the color pattern polymorphism of the Japanese four-lined snake *Elaphe quadrivirgata* are well-examined (Kuriyama et al., 2013). Populations of *E. quadrivirgata* exhibit a pronounced color polymorphism, including striped, pale-striped, nonstriped, banded, and melanistic morphs (Mori et al., 2005; Tanaka and Mori, 2007, Kuriyama et al., 2011, 2013). In a histological study of the pigment cells of the striped, nonstriped, and melanistic morphs of adult *E. quadrivirgata*, Kuriyama et al. (2013) revealed that spatial variation in the abundance and architecture of epidermal and dermal melanophores is a key determinant of

Contract grant sponsor: Grants-in-Aid for Scientific Research from the Ministry of Education, Culture, Sports, Science, and Technology; Grant numbers: 19570026, 21570024, and 15H04426 (to M.H.).

*Correspondence to: Takeo Kuriyama, Department of Environmental Science, Faculty of Science, Toho University, Miyama 2-2-1, Funabashi, Chiba 274-8510, Japan. E-mail: kuriyama.takeo@gmail.com

Received 12 May 2015; Revised 7 September 2015; Accepted 18 October 2015.

Published online 20 November 2015 in Wiley Online Library (wileyonlinelibrary.com).
DOI 10.1002/jmor.20489

differences in stripe vividness between striped and nonstriped phenotypes. Murakami et al. (2014) showed that the stripes of juvenile *E. quadrivirgata* are reddish, but eventually become dark brown in adults. This implies that increased melanophore density converts reddish juvenile stripes to dark brown adult stripes. For this reason, *E. quadrivirgata* is becoming known as an excellent model species to examine pigment cell-based mechanisms of ontogenetic color change.

To understand the differences and similarities in pigment cell mechanisms underlying postembryonic stripe-pattern formation in different morphs, we examined epidermal and dermal pigment cells of newly hatched striped and nonstriped *E. quadrivirgata*, and performed a comparative analysis using published data for adults belonging to the same color morphs (Kuriyama et al., 2013). We quantified these differences by calculating the density of epidermal melanophores as well as dermal xanthophores, iridophores, and melanophores based on transmission electron microscope (TEM) and light microscope images of skin pigment cells. We discuss the relationship between postembryonic and embryonic stripe pattern development as a framework for future studies of the genetic mechanisms of color pattern formation (Murray and Myerscough, 1991; Baker et al., 2009; Chang et al., 2009).

MATERIALS AND METHODS

Elaphe quadrivirgata (H. Boie, 1826) coloration is polymorphic in the population inhabiting Niijima Island of the Izu Islands in Japan (34°22′37″N; 139°15′23″E). Three distinct color morphs are observed in adults: striped, pale-striped, and nonstriped (Kuriyama et al., 2013; Murakami et al., 2014). However, only two color morphs, characterized by the presence and absence of two longitudinal red-brown stripes on the body trunk, have been recognized in juvenile snakes (Murakami et al., 2014; Fig. 1). Four gravid females were collected in June and July 2012, and a total of 25 eggs were obtained. All eggs were incubated in our laboratory at room temperature (25–30°C). Ten hatchlings, including five striped and five nonstriped individuals, were randomly selected for histological analysis.

The positions of two designated dorsal scales were used to compare the vertical architecture of pigment cells between stripe and interstripe background regions. *Elaphe quadrivirgata* has 19 scale rows around the midbody from snout to vent. The scale row along the median dorsal line was designated No. 1, and the fourth scale rows on both sides were each labeled No. 4 (Fig. 1). In a typical striped morph of adult *E. quadrivirgata*, the No. 1 scales are light yellow, and a dark-brown stripe runs over the No. 4 scales (Kuriyama et al., 2013).

After euthanizing the juveniles by excessive inhalation of 100% diethyl ether, a dorsal skin sample was removed from each of 10 juvenile snakes (five striped and five nonstriped morphs). The fresh dorsal skin tissues were observed using a stereomicroscope, a light microscope, and a dark-field epi-illumination microscope. Cross sections of fixed skin tissues were observed using both a light microscope and a TEM. Skin tissue sections measuring 2 mm^3 were sampled from the aforementioned snakes for TEM observations. After fixing the samples in 2.5% glutaraldehyde in 0.1 mol l^{-1} phosphate buffer (pH 7.3) overnight at 4°C, the tissues were rinsed with 0.25 mol l^{-1} sucrose in 0.1 mol l^{-1} phosphate buffer (pH 7.3) and subsequently fixed with 0.1 mol l^{-1} buffer containing 1% osmium tetroxide for 2 h at room temperature. The tissues were thoroughly rinsed with the same buffer solution and then dehydrated using increasing concentrations of ethanol. Finally, the tissues were embedded in epoxy resin (Quetol 651; Okenshoji, Tokyo, Japan). Semithin and ultrathin sections were prepared using a glass or a diamond knife attached to a Porter Blum MT-1 Ultra-microtome (Ivan Sorvall, Newtown, CT). The semithin sections were observed under a light microscope after staining with 1% toluidine blue. The ultrathin sections were double stained with uranyl acetate and alkaline lead and viewed using a JEM-1212 TEM at 80 kV.

The epidermal and dermal pigment cell compositions and architectural structures at No. 1 and No. 4 scales of the two color morphs were characterized and compared between juvenile and adult snakes according to the analytical procedure of Kuriyama et al. (2013). First, the vertical architecture of pigment cells occupying the epidermal and dermal layers was observed in the semithin and ultrathin cross-sections of skin tissue samples. Second, the number of epidermal melanophores was counted, and the proportion of a given vertical area of dermis that was occupied by dermal melanophores was measured using light-microscope photographs of semithin sections along a horizontal distance of 300 μm. Third, the areas occupied by xanthophores and iridophores were measured using TEM photographs of ultrathin sections along a horizontal distance of 10 μm.

Statistical Analysis

The number of epidermal melanophores, the proportion of area occupied by dermal melanophores (per 300 μm of vertical section), and xanthophores and iridophores per 10 μm in Nos. 1 and 4 scales were compared between the two morphs using a generalized linear model with the negative binomial distribution (MASS package in R ver. 3.1.2). The explanatory variables were transformed into binary variables (i.e., dummy variables) with respect to the No. 1 scale for analyses between the scales and the striped morph for analyses between morphs. The effect of the explanatory factor was evaluated based on the *z*-statistic (estimate/SE) and a comparison of Akaike's information criterion (AIC) values between the model and a null model. A *z*-value of greater than 2 or less than −2 indicated that the densities or cell numbers were significantly lower or higher in scale No. 1 or the striped morph than in scale No. 4 or the nonstriped morph. Moreover, if the AIC value of a model with the explanatory variable was less than that of a null model by at least 2, it was evaluated as significant. In both the striped and nonstriped morphs, the number of epidermal melanophores and the area occupied by dermal melanophores were measured using light-microscope photographs of semithin sections along a horizontal distance of 300 μm with ImageJ. The relative area of xanthophores and iridophores that occupied the dermal layer was measured with ImageJ using three electron micrographs taken at 4,000× magnification. The abundances of each epidermal and dermal pigment cell were compared between juveniles and adults, as described by Kuriyama et al. (2013).

All animal work was reviewed and approved by the Toho University Bioethics and Animal Ethics Committee (approval number: #12-51-242).

RESULTS

In the striped juvenile, we observed two red-brown longitudinal dorsal stripes over a yellowish-brown background color (Fig. 1A–D). Cross-bar markings connecting the stripes formed a ladder-like pattern behind the head, but faded toward the posterior part of the body. The nonstriped morph exhibited a uniform brown or light-brown background without a trace of dorsal stripes, except for

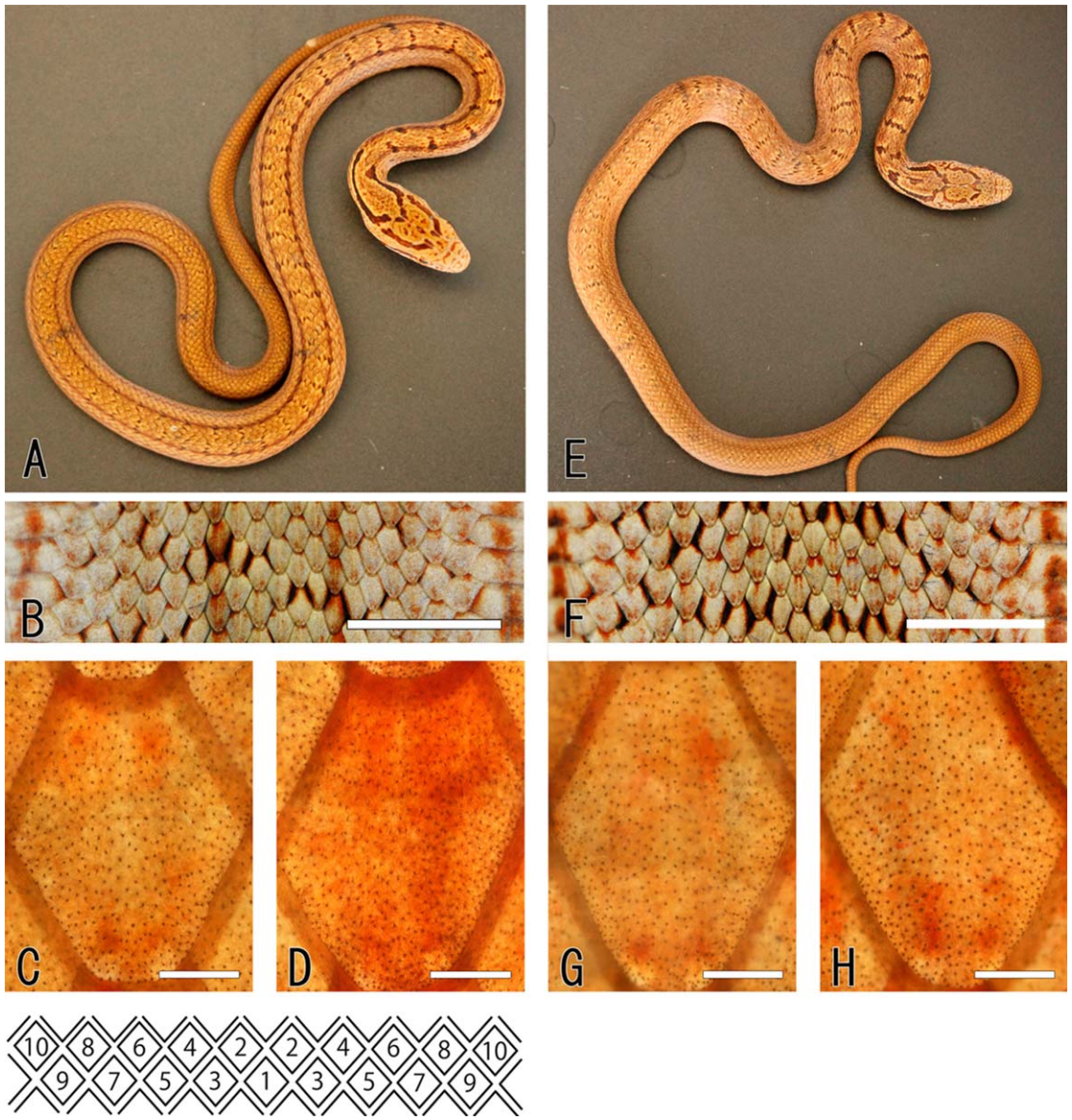

Fig. 1. *Elaphe quadrivirgata*, dorso-lateral views of two color morphs of juveniles. From **A** to **D**: Striped morph. From **E** to **H**: Nonstriped morph. **B** and **F**: Skin removed from individuals. **C**, **D**, **G**, and **F**: The dorsal scale observed using a light microscope in incident light. In a typical striped morph, the No. 1 scales are light yellow, and a dark-brown stripe runs over the No. 4 scales. Bar = 5 mm (Figs. B and F), 0.3 mm (Figs. 1C–E, G, H).

in the region just behind the head (Fig. 1E–H). In the nonstriped morph, cross-bar markings were present only behind the head. The ladder pattern was absent and the size of the cross-bars decreased toward the posterior part of the body.

We examined the fixed tissue cross sections with a light microscope and a TEM and observed four types of pigment cells. These cells were vertically structured in the same order in the epidermal and dermal layers of skin at the Nos. 1 and 4 scales in the striped and nonstriped morphs (Figs. 2–4). All epidermal melanophores were filled with electron-dense oval granules called "melanosomes" that were approximately 0.5 μm in length and 0.2 μm in width (Fig. 3A) and positioned superficial to the basal layer (Fig. 4). In the dermis, we also observed three types of pigment cells: yellow xanthophores, light reflecting iridophores, and black melanophores (Figs. 2–4). Xanthophores containing pterinosomes that were approximately 0.4 μm in diameter and enclosed several membranes were consistently located just below the basal layer of the epidermis, except for one case in which xanthophores were located below the stratum of iridophores in a striped morph skin tissue sample of the No. 4 scale (Figs. 3C and 4). Dermal melanophores contained melanosomes that were approximately 0.6 μm in length and 0.4 μm in width and

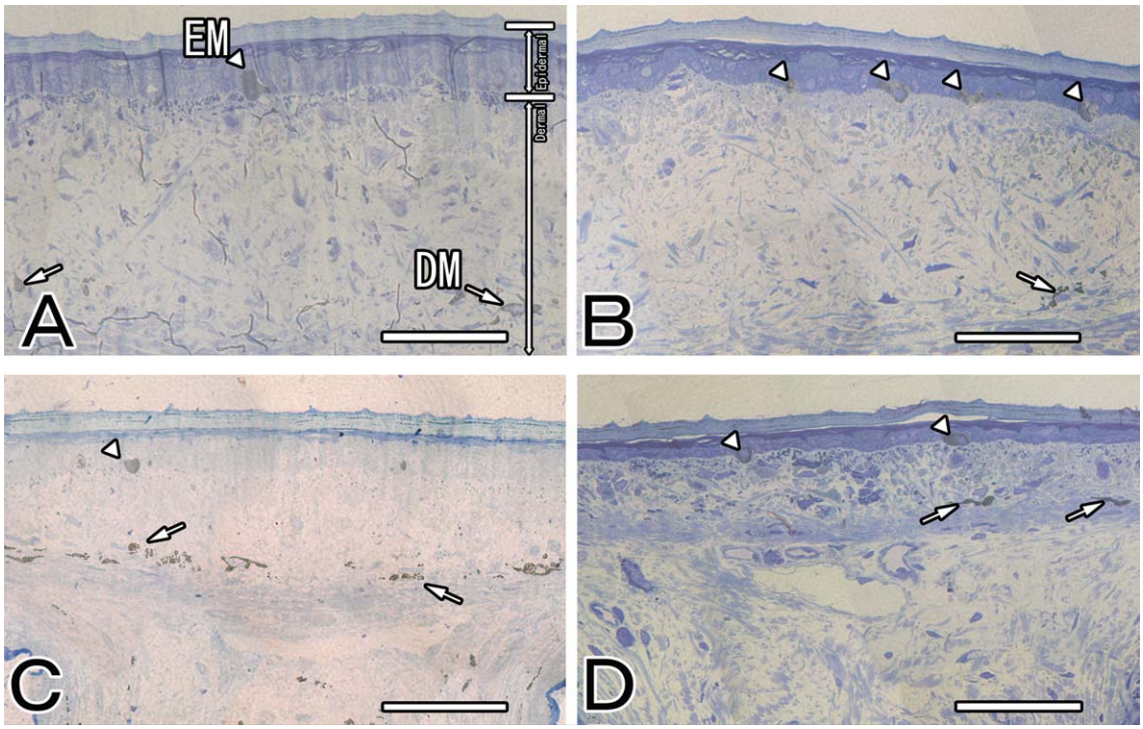

Fig. 2. *Elaphe quadrivirgata*, semithin cross section of the Nos. 1 and 4 dorsal scales of the juvenile striped and nonstriped color morphs. **A**: Yellow background skin of dorsal scale No. 1 of a striped morph. **B**: Dark-brown skin No. 4 scale of a striped morph. **C**: No. 1 scale and **D**: No. 4 scale of a nonstriped morph. Arrowheads and EM indicate epidermal melanophores; Arrow and DM indicate dermal melanophore. Stained with toluidine blue. Bar = 50 μm.

were located at the bottom of the dermal layer (Figs. 3B and 4). Iridophores containing light reflecting platelets were located between the strata of xanthophores and melanophores (Figs. 3D and 4).

Differences in Pigment-Cell Architecture and Density Between Striped and Nonstriped Juveniles

We compared the density of pigment cells occupied by the epidermal and dermal layers between the striped and nonstriped morphs for the scales of the stripe (No. 4) and background regions (No. 1). In the striped morph, the mean density of epidermal melanophores was approximately 3.5 times greater for the No. 4 than No. 1 scales (Tables 1 and 2, Fig. 2A,B). The area of xanthophores in a 10-μm vertical section of the dermis was about two times greater for No. 4 than No. 1 scales (Tables 1 and 2, Fig. 4A,B). The areas occupied by dermal melanophores and iridophores in the 10-μm vertical section of the dermis were not significantly different between Nos. 1 and 4 scales (Tables 1 and 2, Figs. 2A,B and 4A,B).

In the nonstriped morph, the density of dermal melanophores was higher for No. 1 than No. 4 scales (Tables 1 and 2, Fig. 2C,D). The vertical architecture, the number of epidermal melanophores, and the density of iridophores and xanthophores were not statistically different between the Nos. 1 and 4 scales (Tables 1 and 2, Figs. 2C,D and 4C,D).

We compared the abundance and densities of dermal pigment cells in Nos. 1 and 4 scales between the striped and nonstriped morphs. The density of epidermal melanophores and xanthophores in No. 4 scales were about three and two times higher in the striped morph than the nonstriped morph, respectively (Tables 1 and 3). The densities of dermal melanophores and iridophores were not significantly different (Tables 1 and 3). In scale No. 1, the quantities of each epidermal and dermal pigment cell type did not differ significantly between the two morphs (Tables 1 and 3).

Differences in Pigment-Cell Architecture and Density Between Juvenile and Adult Snakes

To characterize the pigment cell mechanisms of ontogenetic color pattern formation, we compared the number of epidermal melanophores, the proportion of dermal melanophores, and the vertical architecture of dermal pigment cells between juveniles (estimated in this study) and adult snakes (Kuriyama et al, 2013). In both the striped and nonstriped morphs, the number of epidermal melanophores and the proportion of dermal melanophores were higher in adult snakes than in juvenile snakes at the Nos. 1 and 4 scales (Table 1).

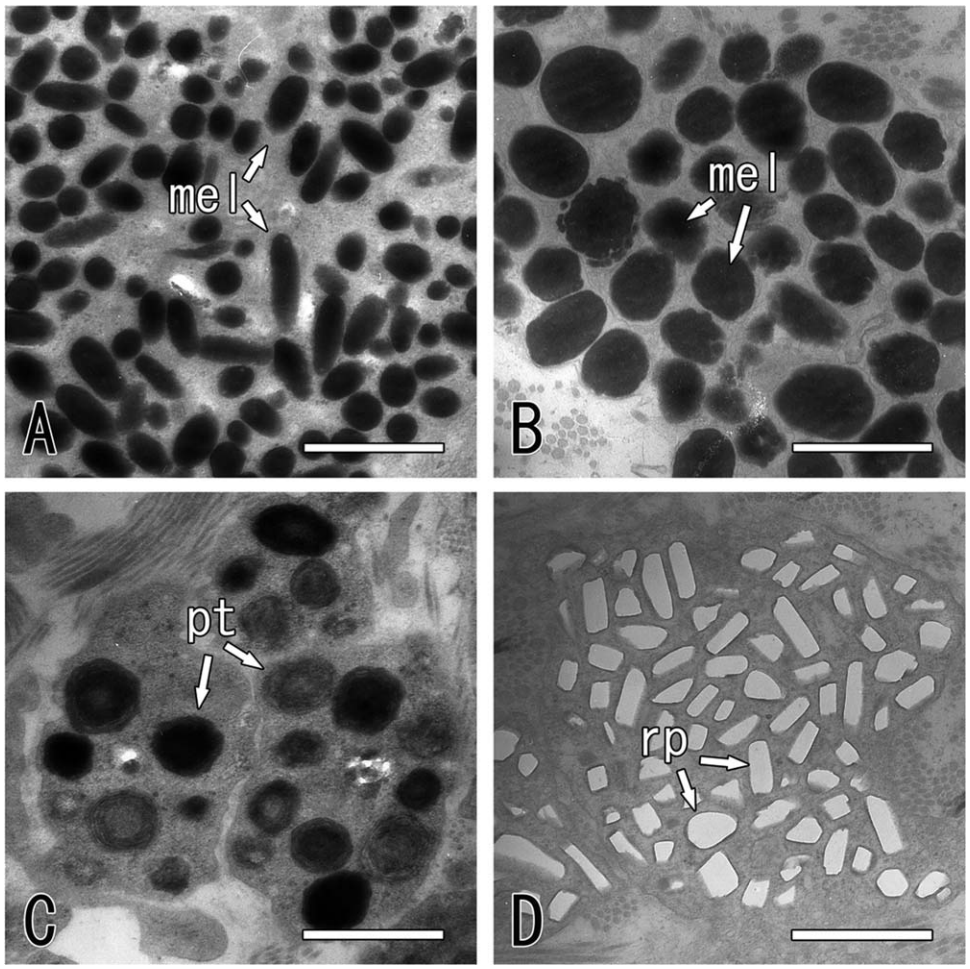

Fig. 3. *Elaphe quadrivirgata*, transmission electron micrograph of four types of epidermal and dermal pigment cells in a No. 4 scale of a nonstriped juvenile. **A**: Epidermal melanophore. **B**: Dermal melanophore. **C**: Xanthophore. **D**: Iridophore. Mel, melanosome; rp, light-reflecting platelets; pt; pterinosome. Bar = 1 μm.

The density of melanophores was much higher in the dermis than in the epidermis in both the striped and nonstriped morphs. From the juvenile to adult stage, the density of dermal melanophores increased by about 8- to 11-fold in the striped morph, and 5- to 10-fold in the nonstriped morph. The density of epidermal melanophores increased from the juvenile to adult stage, with slightly higher increases in the nonstriped (3- to 4-fold) than the striped morph (1.5- to 2.1-fold). The vertical architecture of dermal melanophores in the No. 4 scale changed from a single stratum at the bottom of the dermis in juveniles to double strata both above and below the xanthophores and iridophores in adults. We did not observe any such structural changes in the nonstriped morph.

DISCUSSION

This is the first study to examine the pigment cell composition and their vertical architectures in order to understand ontogenetic color changes in reptilian sauropsids. We found that the ontogenetic change from red-brown stripes in juvenile *E. quadrivirgata* to dark-brown stripes in adults was attained by an increase in melanophore density in both the epidermis and dermis. In the dermal layer, two layers of melanophores were produced via the development of a new melanophore layer above the layers of xanthophores and iridophores. Additionally, we noted that the difference between the striped and nonstriped morphs in the spatial and vertical architectures of epidermal and dermal pigment cells already existed at the timing of hatching, indicating that basic mechanisms for differentiating the striped and nonstriped morphs function during embryonic development.

Kuriyama et al. (2013) concluded that changes in the densities of epidermal and dermal melanophores explain the observed variation in stripe vividness between the striped and nonstriped morphs. Our results were consistent with this inference and with the results of Murakami et al.

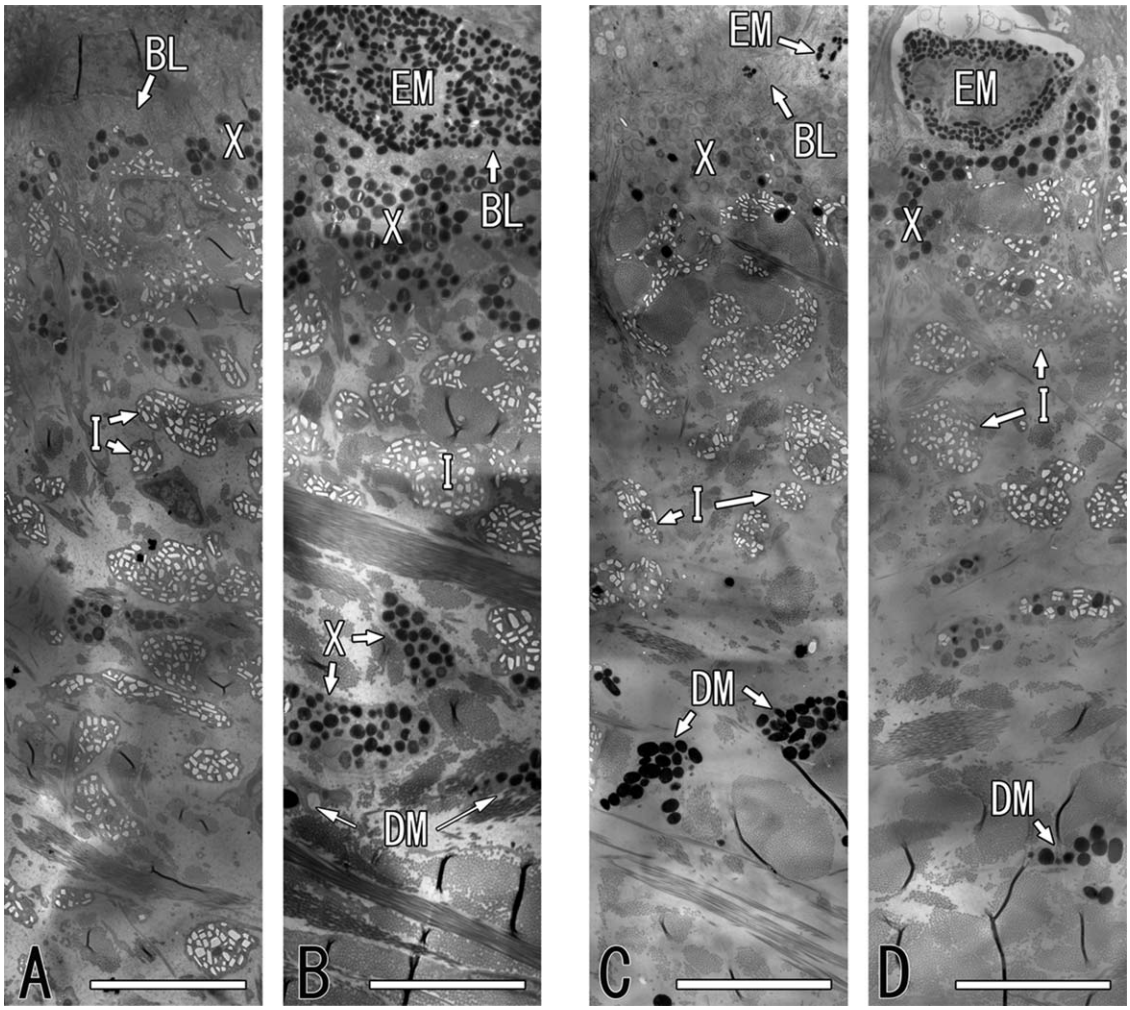

Fig. 4. *Elaphe quadrivirgata*, transmission electron micrograph showing the combination of epidermal and dermal pigment cells in a striped and nonstriped juvenile. **A**: Yellow background skin of a No. 1 scale, and **B**: Dark-brown skin No. 4 scale of a striped morph; epidermal melanophore in the epidermis. The dermal pigment cells showed a vertical combination of xanthophores just below basal lamella, iridophores in the middle and melanophore at the bottom. **C**: No. 1 scale and **D**: No. 4 scale of a nonstriped morph. The vertical combination of epidermal and dermal pigment cells in No. 1 and No. 4 were same as striped morph. EM, epidermal melanophore; X, xanthophore; I, iridophore; DM, dermal melanophore; BL, basal lamella. Bar = 5 μm.

(2014); spatial variation in the abundance and architecture of epidermal and dermal melanophores is the key pigment-cell mechanism that explains variation in stripe vividness. Specifically, the contrast in spatial densities of epidermal and dermal melanophores increased from the juvenile

TABLE 1. Densities of pigment cells in both juvenile and adult Elaphe quadrivirgata skin tissues. Densities of epidermal and dermal melanophores of adult snake are described in Kuriyama et al. (2013). Values indicate means ± SD

		Number of epidermal melanophore	Proportion of melanophore in dermis	Density of xanthophore (μm^2)	Density of iridophore (μm^2)
Juvenile					
Striped	Scale 1	1.20 ± 0.75	0.017 ± 0.009	19.12 ± 4.93	70.03 ± 18.51
	Scale 4	4.20 ± 2.32	0.017 ± 0.008	37.10 ± 6.38	55.91 ± 28.22
Nonstriped	Scale 1	1.00 ± 0.00	0.019 ± 0.011	25.03 ± 6.57	61.51 ± 19.25
	Scale 4	1.40 ± 0.49	0.010 ± 0.004	19.88 ± 9.14	68.44 ± 17.96
Adults					
Striped	Scale 1	2.50	0.13	—	—
	Scale 4	6.92	0.19	—	—
Nonstriped	Scale 1	4.17	0.10	—	—
	Scale 4	4.33	0.10	—	—

*TABLE 2. Comparison of the number of epidermal melanophores, the proportion of the area occupied by dermal melanophores (per 300 μm of vertical section), and xanthophores and iridophores per 10 μm in Nos. 1 and 4 scales of each morph using a generalized linear model with the negative binomial distribution. * indicates z-value of greater than 2 or less than −2*

				Scale No. 1			Intercept		
			AIC	Estimate	SE	*z*	Estimate	SE	*z*
Number of epidermal melanophore	Striped		41.4	−1.3	0.5	−2.6*	1.4	0.2	6.2
		Null	45.6	—	—	—	1.0	0.3	3.7
	Nonstripe		28.1	−0.3	0.6	−0.6	0.3	0.4	0.9
		Null	26.4	—	—	—	0.2	0.3	0.6
Proportion of dermal melanophore in dermis	Striped		136.8	0.0	0.4	0.0	−4.1	0.3	−13.9
		Null	128.7	—	—	—	5.6	0.2	36.1
	Nonstripe		124.3	0.6	0.3	2.1*	−4.6	0.2	−21.3
		Null	128.1	—	—	—	5.4	0.2	27.3
Density of xanthophore	Striped		69.1	−0.7	0.1	−4.9*	3.6	0.1	44.6
		Null	79.4	—	—	—	3.3	0.1	27.2
	Nonstripe		77.1	0.2	0.2	1.0	3.0	0.2	17.0
		Null	75.9	—	—	—	3.1	0.1	24.3
Density of iridophore	Striped		102.0	0.2	0.3	0.7	4.0	0.2	17.7
		Null	100.5	—	—	—	4.1	0.2	25.2
	Nonstripe		92.0	−0.1	0.2	−0.6	4.2	0.1	33.7
		Null	90.4	—	—	—	4.2	0.1	45.9

to adult stages. The sharpness of the boundary between the dark- and light-colored scales increased in the striped morph, but the density of melanophores increased to a greater extent in the dermis than the epidermis in both morphs. During postembryonic development, the densities of epidermal and dermal melanophores increased in both the striped and nonstriped morphs. However, a double stratum of dermal melanophores only developed in the scales of the dark-brown stripes of the striped morph.

Kuriyama et al. (2013) proposed that the alleles responsible for stripe pattern formation control the distribution and density of melanophores, and that these alleles have an additive effect on stripe vividness. This conjecture is based on the hypothesis that allele for the striped morph is dominant over the allele for the nonstriped morph under a model of incomplete dominance heredity for one locus with two alleles. The observed frequencies of striped and nonstriped neonates that hatched from clutches laid by striped, pale-striped, and nonstriped females support this pattern of inheritance (Murakami et al., 2014).

To further improve our understanding of color pattern formation in reptilian sauropsids, future studies will examine changes in these patterns during embryonic development. Based on the hypothesis that color patterning mechanisms are established during embryonic development, these studies will determine the timing of melanophore, xanthophore, and iridophore patterning formation during

*TABLE 3. Comparison of the number of epidermal melanophores, the proportion of the area occupied by dermal melanophores (per 300 μm of vertical section), and xanthophores and iridophores per 10 μm in Nos. 1 and 4 scales between striped and nonstriped morphs using a generalized linear model with the negative binomial distribution. * indicates z-value of greater than 2 or less than −2*

				Striped morph			Intercept		
			AIC	Estimate	SE	*z*	Estimate	SE	*z*
Number of epidermal melanophore	Scale 1		28.6	0.2	0.6	0.3	0.0	0.4	0.0
		Null	26.7	—	—	—	0.1	0.3	0.3
	Scale 4		41.0	1.1	0.4	2.5*	0.3	0.4	0.9
		Null	44.7	—	—	—	1.0	0.2	4.3
Proportion of dermal melanophore in dermis	Scale 1		135.6	−0.1	0.4	−0.3	−3.9	0.3	−15.3
		Null	128.2	—	—	—	5.7	0.1	39.9
	Scale 4		126.5	0.5	0.4	1.4	−4.6	0.3	−17.9
		Null	126.9	—	—	—	5.3	0.2	26.6
Density of xanthophore	Scale 1		69.1	−0.3	0.2	−1.6	3.2	0.1	28.7
		Null	69.4	—	—	—	3.1	0.1	33.4
	Scale 4		79.3	0.6	0.2	2.9*	3.0	0.2	18.8
		Null	83.2	—	—	—	3.4	0.1	22.5
Density of iridophore	Scale 1		92.3	0.1	0.2	0.7	4.1	0.1	32.3
		Null	90.8	—	—	—	4.2	0.1	45.5
	Scale 4		101.8	−0.2	0.3	−0.7	4.2	0.2	18.8
		Null	100.2	—	—	—	4.1	0.2	25.3

embryonic stages. Additional analyses of the temporal and spatial pattern of candidate gene expression will facilitate the identification of genes responsible for color pattern formation and their roles in the differentiation, movement, proliferation, and death of pigment cells (Murray and Myerscough, 1991; Baker et al., 2009; Chang et al., 2009).

Studying stripe pattern formation during embryonic development is fundamental to improve our understanding of the processes and mechanisms of pigment cell differentiation and the spatial configuration of those pigment cells. Using stripe formation during the embryonic development of zebrafish as a model, various mechanisms have been inferred: undifferentiated stem cells migrate to a specific part of the body trunk and are transformed into mature pigment cells; mature pigment cells aggregate at a specific body part and proliferate at a greater rate than those in other parts of the embryonic body; or, complex combinations of cell differentiation, migration, and proliferation produce a particular color pattern (e.g., Kelsh et al., 2009; Parichy and Spiewak, 2014). We observed little or no difference in the density of epidermal and dermal melanophores in juveniles and adults of the nonstriped morph, suggesting that the mechanisms governing the spatial concentration of melanophores are important for stripe pattern formation. Therefore, we are currently evaluating color pattern formation in embryonic development and gene expression analyses to determine the mechanisms of pigment cell differentiation and the maintenance of the spatial configuration of mature pigment cells (Kelsh et al., 2009; Higdon et al., 2013; Parichy and Spiewak, 2014).

ACKNOWLEDGMENTS

The authors thank M. Aoki, M. C. Brandley, Y. Isaka, Y. Kanamori, M. Kuroe, T. Okamoto, S. Takagi, and T. Tanaka for assisting field work. We received technical guidance of a light microscope and TEM from M. Sugimoto and M. Ohata. We would like to express sincere thanks to M. C. Brandley for his reading and improvement of the manuscript.

LITERATURE CITED

Alibardi L. 2011. Histology, ultrastructure, and pigmentation in the horny scales of growing crocodilians. Acta Zool 92:187–200.

Alibardi L. 2012. Cytology and localization of chromatophores in the skin of the Tuatara (*Sphenodon punctaus*). Acta Zool 93:330–337.

Allen WL, Baddeley R, Scott-Samuel NE, Cuthill IC. 2013. The evolution and function of pattern diversity in snakes. Behav Ecol 24:1237–1250.

Baker RE, Schnell S, Maini P. 2009. Waves and patterning in developmental biology: Vertebrate segmentation and feather bud formation as case studies. Int J Dev Biol 53:783–794.

Bechtel HB. 1978. Color and pattern in snakes (Reptilia, Serpentes). J Herpetol 12:521–532.

Chang C, Wu P, Baker RE, Maini PK, Alibardi L, Chuong CM. 2009. Reptile scale paradigm: Evo-Devo, pattern formation and regeneration. Int J Dev Biol 53:813–826.

Cooper WEJ, Greenberg N. 1992. Reptilian coloration and behavior. In: Gans C, Crews D, editors. Biology of the Reptilian, Vol. 18: Hormones, Brain, and Behavior. Chicago: The University Chicago Press. pp 298–422.

Higdon CW, Mitra RD, Johnson SL. 2013. Gene expression analysis of zebrafish melanocytes, iridophores, and retinal pigmented epithelium reveals indicators of biological function and developmental origin. PLoS ONE 8:e67801.

Kelsh RN, Harris ML, Colanesi S, Erickson CA. 2009. Stripes and belly-spots—A review of pigment cell morphogenesis in vertebrates. Semin Cell Dev Biol 20:90–104.

Kronforst MR, Barsh GS, Kopp A, Mallet J, Monteiro A, Mullen SP, Protas M, Rosenblum EB, Schneider CJ, Hoekstra HE. 2012. Unraveling the thread of nature's tapestry: The genetics of diversity and convergence in animal pigmentation. Pigment Cell Melanoma Res 25:411–433.

Kuriyama T, Miyaji K, Sugimoto M, Hasegawa M. 2006. Ultrastructure of the dermal chromatophores in a lizard (Scincidae: *Plestiodon latiscutatus*) with conspicuous body and tail coloration. Zool Sci 23:793–799.

Kuriyama T, Brandley MC, Katayama A, Mori A, Honda M, Hasegawa M. 2011. A time-calibrated phylogenetic approach to assessing the phylogeography, colonization history and phenotypic evolution of snakes in the Japanese Izu Islands. J Biogeogr 38:259–271.

Kuriyama T, Misawa H, Miyaji K, Sugimoto M, Hasegawa M. 2013. Pigment cell mechanisms underlying dorsal color-pattern polymorphism in the Japanese four-lined snake. J Morphol 274:1353–1364.

Mori A, Tanaka K, Moriguchi H, Hasegawa M. 2005. Color variation in *Elaphe quadrivirgata* throughout Japan. Jpn J Herpetol 2005:22–38. (In Japanese)

Morrison RL. 1995. A transmission electron microscopic (TEM) method for determining structural colors reflected by lizard iridophores. Pigment Cell Res 8:28–36.

Murakami A, Hasegawa M, Kuriyama T. 2014. Identification of juvenile color morphs for evaluating a heredity model of stripe/non-stripe pattern polymorphism in the Japanese four-lined snake *Elaphe quadrivirgata*. Curr Herpetol 33:68–74.

Murray JD, Myerscough MR. 1991. Pigmentation pattern formation on snakes. J Theor Biol 149:339–360.

Olsson M, Stuart-Fox D, Ballen C. 2013. Genetics and evolution of colour patterns in reptiles. Semin Cell Dev Biol 24:529–541.

Parichy DM, Spiewak JE. 2014. Origins of adult pigmentation: Diversity in pigment stem cell lineages and implications for pattern evolution. Pigment Cell Melanoma Res 28:31–50.

Saenko S, Teyssier J, van der Marel D, Milinkovitch M. 2013. Precise colocalization of interacting structural and pigmentary elements generates extensive color pattern variation in *Phelsuma* lizards. BMC Biol 11:105.

Tanaka K, Mori A. 2007. Quantitative evaluation of individual snake coloration by use of principal components analysis with variable selection. Curr Herpetol 26:117–137.

Wilson D, Heinsohn R, Endler JA. 2007. The adaptive significance of ontogenetic colour change in a tropical python. Biol Lett 3:40–43.

Wolf M, Werner YL. 1994. The striped color pattern and striped/non-striped polymorphism in snakes (Reptilia: Ophidia). Biol Rev 69:599–610.